Autonomous time and phase calibration of spaceborne bistatic SAR systems

Marc Rodriguez-Cassola, German Aerospace Center, marc.rodriguez@dlr.de, Germany
Pau Prats-Iraola, German Aerospace Center, pau.prats@dlr.de, Germany
Paco López-Dekker, German Aerospace Center, francisco.lopezdekker@dlr.de, Germany
Andreas Reigber, German Aerospace Center, andreas.reigber@dlr.de, Germany
Gerhard Krieger, German Aerospace Center, gerhard.krieger@dlr.de, Germany
Alberto Moreira, German Aerospace Center, alberto.moreira@dlr.de, Germany

Abstract

Bistatic and multistatic SAR constellations offer increased performance at the expense of increased operational complexity. Due to geometric or cost constraints, multistatic SAR constellations might be forced to operate in a partially cooperative manner, i.e., without a direct synchronisation link. In demanding scenarios, like high-resolution bistatic SAR imaging or cross-platform SAR interferometry or tomography, the data need undergo a calibration step to compensate the lack of synchronisation between transmitter and receiver master clocks. Autonomous synchronisation, based on the inversion of the phase and positioning errors of the bistatic SAR images caused by the lack of synchronisation, is used to calibrate the time and phase references of the system with the sole help of the received radar data, which drastically reduces the requirements on the hardware of the system.

1 Introduction

The lack of synchronisation, caused by the operation of transmitter and receiver with different master clocks, poses one of the fundamental operational problems of bistatic radars. The frequency difference of these clocks scales to the operational frequencies of the bistatic radar electronics, destroying the absolute time (range) and phase (Doppler) references of the system. In general, synchronous radar operation requires the use of the same clock reference, a condition fulfilled by monostatic SARs, but not by bistatic SARs. Due to the performance decrease caused by the use of different clocks, the design of strategies for effective synchronisation is an essential research topic among bistatic radar engineers [1]. In particular, the development of processing algorithms to estimate and compensate clock phase errors from the acquired bistatic data is especially attractive, since it relaxes the hardware requirements by minimising the need for clock information exchange between transmitter and receiver and reduces the overall cost of the system.

Due to geometric or cost constraints, future multistatic SAR constellations might be forced to operate in partially cooperative manner, i.e., without the help of a direct synchronisation link. The very first problem partially cooperative bistatic systems have to face is valid data acquisition at all, especially if the receiver has a limited data rate. There exist several methods to solve this, e.g., the inclusion of a detector to trigger the echo window [2], the use of an external time reference (i.e., GNSS signal) [3], or the prolongation of the echo window length [4]. The precision required for the synchronisation of the echo window is usually modest, in the order of tenths of microseconds. An accurate time and phase synchronisation of the bistatic data, i.e., a robust and accurate matching of transmitter and receiver clock phases, with random mean errors definitely smaller than a fraction of a wavelength, is however a much stricter requirement. Most present SAR applications require calibrated measurements both in amplitude and phase, with typical accuracies of about 0.5 dB and 10 deg, respectively. In non-synchronous operation, these values might be hardly achieved if accurate synchronisation is not available. Autonomous synchronisation has been used in the evaluation of data acquired in cross-platform bistatic interferometric experiments like the DLR-ONERA bistatic experiment [5] and the first experimental cross-platform interferograms with TanDEM-X during the pursuit monostatic commissioning phase [6].

2 Effects of lack of synchronisation

2.1 Clock error model

The clock phase error in bistatic SAR is defined as the difference in the master oscillator phase output between transmitter and receiver. SAR master clocks usually have a very good short-term stability, i.e., the low-frequency components of the oscillator phase noise cancel out after demodulation [1]. Consequently, the oscillator phase error in monostatic SAR systems is limited to the high-frequency components of the phase noise of the master clock. This cancellation does not occur in bistatic systems, where in addition to low and high-frequency phase noise components, any other deterministic offsets add up. Accurate descriptions of the quality of oscillators can be found in the classic literature [7], from which specific characterisations of SAR master clocks have already been

derived [1, 8]. In the following, the clock error during the time of the bistatic acquisition is modelled as follows

$$\delta\phi_{\mathrm{clock}}(t) = \delta\phi_{0,\mathrm{clock}} + 2\pi \cdot \int_{t_0}^{t} \mathrm{d}\tau \cdot \delta f_{0,\mathrm{clock}}(\tau) \quad , \quad (1)$$

where t is the absolute time, t_0 is the start time at which both clocks started drifting apart, and $\delta f_{0,\mathrm{clock}}(t)$ is a stationary process which represents the instantaneous frequency offset between transmitter and receiver master clocks. Variable t represents both fast and slow time components. All frequencies of the radar are derived from the master oscillator after proper multiplication/division procedures. We assume that the scaling of the frequencies neither breaks the stationarity of the processes nor changes the form of their power spectral density, other than scaling the statistical moments accordingly. For compactness, $\delta f_{0,\mathrm{clock}}$ is assumed in the following to be scaled to the carrier frequency of the radar.

2.2 Effect on the single pulse

In the case of a chirp of chirp rate β_{r}, the received phase can be expressed as

$$\phi_{\mathrm{s}}(t_{\mathrm{r}}) \approx -\pi \cdot \frac{\beta_{\mathrm{r}} + \delta\beta_0}{\mu_{\mathrm{c}}^2} \cdot \left(t_{\mathrm{r}} - \frac{\mu_{\mathrm{c}} \cdot \delta f_0}{\beta_{\mathrm{r}} + \delta\beta_0} \right)^2 - \frac{\pi \cdot \delta f_0^2}{\beta_{\mathrm{r}} + \delta\beta_0} \quad (2)$$

$$\text{with } \mu_{\mathrm{c}} \approx 1 + \frac{\lambda}{\mathrm{c}} \cdot \delta f_0 \quad , \quad (3)$$

where t_{r} is the fast time, c is the velocity of propagation of the transmitted signal, λ is the carrier wavelength, and δf_0 and $\delta\beta_0$ the linear and quadratic components of the clock phase error for the duration of the pulse. From (2), the change in chirp rate, delay, and phase of the received chirp can be identified, i.e., after range compression, the detected chirp will be delayed, slightly defocused and with a phase error. The expected value of δf_0 depends on the characteristics of the systems. If the master oscillators of transmitter and receiver are trimmed before flight, small values can be expected. In the case of TanDEM-X, δf_0 is in the order of hundreds of Hz. In fully non-cooperative scenarios like the hybrid experiment between TerraSAR-X and F-SAR [4], the value of δf_0 was of about 20 kHz. In both cases, the effect of the sampling jitter is negligible, i.e., $\mu_{\mathrm{c}} \approx 1$. Similarly, defocussing is expected to be negligible, as well as the overall phase error of the compressed peak, about 0.03 deg for the cited case. The additional delay is in the order of several nanoseconds.

2.3 Bistatic SAR impulse response

Once the impact of the clock phase errors on the single transmitted pulses has been established, we can write the bistatic SAR impulse response with missing synchronisation as follows

$$h = s_{\mathrm{Tx}}\left(t_{\mathrm{r}} - \frac{r(t_{\mathrm{a}})}{\mathrm{c}} + \delta t_{\mathrm{r,clock}}(t_{\mathrm{a}}) \right) \cdot \exp\left[-\mathrm{j} \cdot \frac{2\pi}{\lambda} \cdot r(t_{\mathrm{a}}) + \mathrm{j} \cdot \delta\phi_{\mathrm{clock}}(t_{\mathrm{r}}, t_{\mathrm{a}}) \right] \quad , \quad (4)$$

where t_{a} is the slow time, $r(t_{\mathrm{a}})$ is the bistatic range history; the assumption of carrier demodulation has been implicitly accepted in (4). The range curvature error, $\delta t_{\mathrm{r,clock}}$ is mainly caused by the difference in the effective PRFs of transmitter and receiver, and can be approximated by

$$\delta t_{\mathrm{r,clock}}(t) \approx \delta t_{\mathrm{r},0} + \frac{\delta f_{0,\mathrm{clock}}(t)}{\beta_{\mathrm{r}}} + \frac{\lambda \cdot [\delta\phi_{\mathrm{clock}}(t) - \delta\phi_{\mathrm{clock}}(t_0)]}{2\pi \cdot \mathrm{c}} \quad ; \quad (5)$$

where the acquisition is assumed to start at time t_0, and $\delta t_{\mathrm{r},0}$ is difference between the start time of the acquisition for transmitter and receiver. The effect of the missing synchronisation in the bistatic SAR impulse response is clear: on one hand, the term $\delta t_{\mathrm{r,clock}}$ alters the range signature of the target; on the other, the term $\delta\phi_{\mathrm{clock}}$ modifies its Doppler signature. Unless synchronisation is achieved, the mismatch in the SAR focussing kernel will distort the reconstructed bistatic SAR image.

2.4 Time and phase synchronisation

As previously discussed, the effect of using different clocks in a bistatic SAR causes a two-dimensional phase error on the bistatic data, which, if not corrected, causes defocussing, positioning and phase errors in the reconstructed images. If the clock phase error between transmitter and receiver is known, the bistatic data can be synchronised on ground in processing stages.

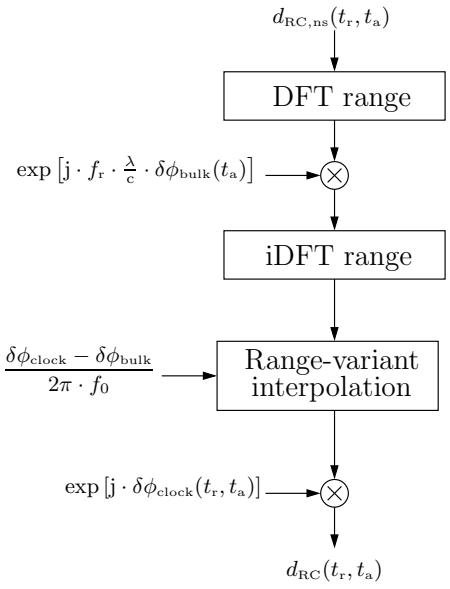

Figure 1: Time and phase synchronisation of the bistatic SAR data. Subindices RC and ns stand for range compressed and non-synchronised, respectively.

Assuming the available clock phase error is 2D, the block diagram of the correction algorithm is depicted in Fig. 1, where $\delta\phi_{\text{bulk}}(t_{\text{a}})$ is a mean value of the phase error for the considered interval between two echo windows.

3 Autonomous estimation of the clock phase error

Automatic synchronisation algorithms estimate the positioning and phase distortions on the bistatic SAR images. Getting advantage of the diversity in range, these distortions are inverted into an estimate of the clock phase error, which can be further used to achieve better synchronisation of the bistatic data. The approach works in an iterative manner. The quality of the estimate, as expected, strongly depends on the quality and quantity of residual phase error measurements available within the image. Two approaches for the automatic estimation of clock phase errors are discussed in this section.

3.1 Autonomous estimation with autofocus

The phase error estimation is performed using autofocus on a single bistatic SAR image. Autofocus algorithms rely on the presence of some kind of contrast within the image, i.e., synchronisation might be difficult to achieve in homogeneous scenes. Whether they rely on the presence of point-like scatterers or not, we will consider two classes of autofocus algorithms: phase-gradient (PGA) or map-drifts (MDA). The former are based on the detection and analysis of the phase errors of point targets of opportunity [4]. The latter rely on the contrast of the images and can use extended and partially distributed targets [9]. The choice between one or the other depends on the kind of scene being imaged. Usually, PGA perform nicely in urban and human-made areas. In general, $\delta\phi_{\text{clock}} - \delta\phi_{0,\text{clock}}$ can be estimated, even $\delta\phi_{\text{clock}}$ if calibrated targets are available. The quality of the estimate depends on the signal-to-clutter ratio (SCR) of the targets. MDA on the other hand can be used on both urban and land areas, with a penalty in the accuracy of the local estimate of the error; using map-drift autofocus, only the derivative of $\delta f_{0,\text{clock}}$ is observable. For the case of a spaceborne bistatic system, and assuming a PGA approach, the standard deviation of the clock phase error estimate can be approximated as follows

$$s_{\phi}[n_{\text{a}}] \approx \frac{1}{I[n_{\text{a}}]^2} \cdot \sum_{i=0}^{I[n_{\text{a}}]-1} \left(\frac{k_1}{\sqrt{\text{SCR}_i}} + \frac{k_2}{\text{SCR}_i} \right), \quad (6)$$

where n_{a} is the discrete slow time variable, $I[n_{\text{a}}]$ is the number of targets of opportunity available for averaging, each having a signal-to-clutter ratio SCR_i, and k_1 and k_2 are constants with values 0.673 and 0.344, respectively. The use of two to three coherent scatterers with SCRs of about 15 dB already allows an estimation of the instantaneous clock error phase better than 5 deg.

3.2 Autonomous estimation using a reference image

We will assume that an error-free reference image is available. Note that this is the case of any single-pass bistatic interferometric system, e.g., TanDEM-X [3]. The estimation of clock phase error is based on the previous estimation of the distortion map of the bistatic SAR image with respect to the reference. Note that a method based on the estimation of the coregistration offsets strongly depends on the observation geometry of the two images, i.e., they must be close enough so that these coregistration offsets can be measured using the image amplitude or the preferred complex information. High SNR or coherence between the images are not required, but improve the estimation of the coregistration offsets. Both range and azimuth positioning errors can be used in the estimation. However, in typical cases, the sensitivity of the azimuth offsets to phase perturbations is significantly higher. In this case, the observable is $\delta f_{0,\text{clock}}$, i.e., an integration step is required to retrieve the phase error. The advantages of this method when compared to the autofocus approach are clear. On one hand, not only point-like, but also extended, and even distributed targets if both images are coherent, can be used for the phase error estimate, thus improving quality and robustness. The standard deviation of the differential clock phase error estimate can be expressed as

$$s_{\phi}(t_{\text{a}}) \approx \frac{4\pi \cdot k_t}{\lambda \cdot \sqrt{\sum_i a_2^{-2}(r_i)}} \cdot \sqrt{t_{\text{a}}}\,, \quad (7)$$

where a_2 is the quadratic component of the bistatic range history and k_t is the accuracy with which the corregistration offsets are measured. Eq. (7) takes the form of a random walk, i.e., errors in the derivative propagate during integration steps, thus increasing the variance of the estimator for long image sizes -the term $\sqrt{t_{\text{a}}}$ in (7)-. The standard deviation of the bistatic range can be derived as follows

$$s_{t_{\text{r}}} \approx k_t \cdot \sqrt{\frac{2}{\text{c}^2 \cdot \sum_i a_2^{-2}(r_i)} \cdot \frac{1}{B_{\text{a}}^2} + \frac{1}{B_{\text{r}}^2 \cdot T_{\text{a}}}} \quad (8)$$

where B_{a} is the azimuth bandwidth, B_{r} is the range bandwidth, and T_{a} the duration of the scene. In practical cases, however, a limit to the variance of the clock phase estimation can be derived by scaling (8) to phases. For a typical TanDEM-X acquisition with a expected coherence between monostatic and bistatic images of 0.9, the degradation of the standard deviation of the phase estimator takes a value of about 0.5 deg/s. In the case of cooperative spaceborne systems, autonomous synchronisation can be used as a back-up solution or to minimise the interruption frequency of a direct link (SyncLink); since the duration of the integration step is limited to the interruption interval, i.e., the value of (7) is bounded. For a typical TanDEM-X case, even in the case of low coherences, a frequency of the synchronization link of about 5 Hz is enough to synchronise the phase of the data autonomously with an accuracy better than 1 deg.

Fig. 2 shows an example of synchronization using a non-coherent image as a reference. The figure corresponds to the first TanDEM-X bistatic acquisition, carried out over Brasilia on August 8th 2010. The along-track baseline between TerraSAR-X and TanDEM-X was of 20 km, i.e., no spectral overlap nor coherence between the monostatic and the bistatic images was expected. Eleven days later, the acquisition was repeated. With the two passes, bistatic repeat-pass interferograms were computed. The figure shows the result (top) before and (bottom) after autonomous synchronization. The azimuthal fringes of the top interferogram are due to the differential clock frequency change between the two passes.

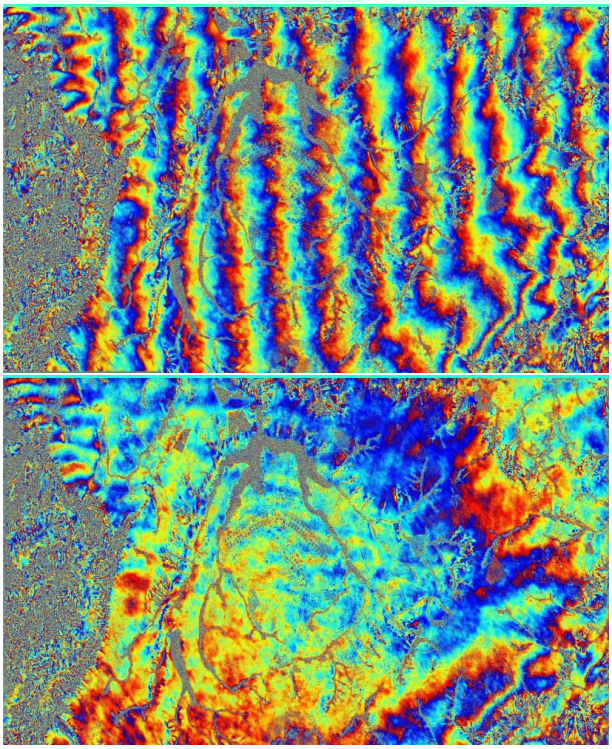

Figure 2: Results of bistatic 11-days repeat-pass interferometry with TanDEM-X (top) before and (bottom) after autonomous synchronization.

As further example with TanDEM-X, corresponding to the bistatic commissioning phase (i.e., with the satellites in close formation with a baseline of only several hundred metres) over *Salar de Uyuni*, Chile. The synchronisation link was normally operated during the acquisition, i.e., a direct reference of the clock phase error is available. We compare then the SyncLink values with those of the autonomous synchronisation (AutoSync). The results of this comparison are shown in Fig. 3, with the dotted line corresponding to the phase measured using the synchronisation link, and the solid being the one estimated using the automatic synchronisation. The difference between both curves is well under 1 deg, which confirms the validity of the approach.

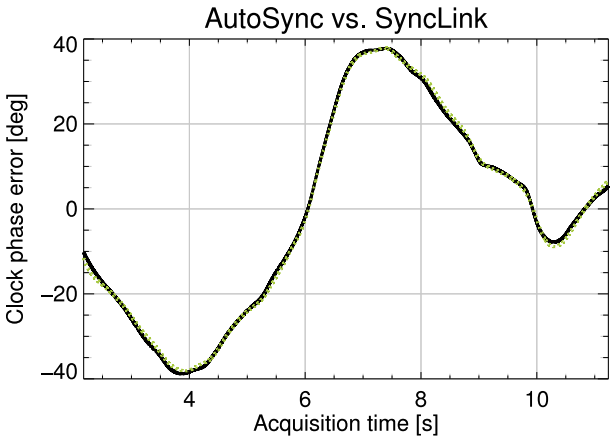

Figure 3: Comparison of estimated clock phase errors, TanDEM-X synchronisation link (dotted) vs. autonomous synchronisation (solid).

4 Conclusion

Autonomous synchronisation can be used to calibrate the time and phase references of future bistatic spaceborne SAR systems with the sole help of the acquired radar data, thus reducing the costs and requirements on the hardware of the system.

References

[1] J. L. Auterman, *Phase stability requirements for bistatic SAR* Proc. IEEE Nat. Radar Conf., USA, 1984.

[2] D. Martinsek and R. Goldstein, *Bistatic radar experiment* Proc. EUSAR, Berlin, 1998.

[3] G. Krieger *et al.*, *TanDEM-X: a satellite formation for high-resolution SAR interferometry* IEEE TGRS, nov. 2007.

[4] M. Rodriguez-Cassola *et al.*, *Bistatic TerraSAR-X/F-SAR spaceborne-airborne SAR experiment: description, data processing and results* IEEE TGRS, feb. 2010.

[5] H. Cantalloube *et al.*, *Challenges in SAR processing for airborne bistatic acquisitions,* Proc. EUSAR, Ulm, 2004

[6] M. Rodriguez-Cassola *et al.*, *First bistatic spaceborne SAR experiments with TanDEM-X* IEEE GRSL, jan. 2012.

[7] J. Rutman, *Characterization of phase and frequency instabilities in precision frequency sources: fifteen years of progress* Proc. IEEE, 1978.

[8] N. Willis, *Bistatic radar*, Artech House, 1991.

[9] H. Cantalloube *et al.*, *Multiscale Local Map-Drift-Driven Multilateration SAR Autofocus Using Fast Polar Format Image Synthesis* IEEE TGRS, oct. 2011.